5-2023

Characterizing the Influence of the MoC Support for the Pt Single Atom Catalyst for the Water Gas Shift Reaction

Kathryn McGee

Characterizing the Influence of the MoC Support for the Pt Single Atom Catalyst for the Water Gas Shift Reaction

Kathryn McGee

Department of Chemical and Biomolecular Engineering, Clemson University

Abstract

In this report, we looked at characterizing the effect of the support (MoC) for the water gas shift (WGS) environment. The single-atom catalyst analyzed was platinum supported in molybdenum carbide. The primary focus of this report was CO* because of the strong interest in using the WGS reaction to convert CO* contamination. All calculations were performed using the density functional theory (DFT) method. We analyzed the binding energies for the different adsorbates, with a special emphasis on CO and charges of the support. We compared our results to Pt/Al_2O_3 support. We observed that the support, specifically MoC participates in the WGS reaction.

Table of Contents

Introduction

This report looks into characterizing the effect of the support by analyzing the adsorbates of the water gas shift (WGS) reaction ($CO + H_2O \leftrightarrow CO_2 + H_2$). The WGS reaction is essential to many industrial processes due to the strong interest in using this reaction to convert CO* contamination[1]. This reaction is of interest primarily for its use in fuel-cell applications[2] and biomass conversion[3]. Using a metal catalyst like platinum (Pt) promotes the reaction in a lower temperature range of 400-573 K[2]. This report looks into CO*, H_2O*, CO_2*, H* because they are relevant catalytic species for water gas shift reaction. The catalyst used in this investigation was Pt on an α-MoC (111) surface. This paper primarily focuses on the CO* because we want to reduce the CO* binding strength to Pt. All calculations were done using the density functional theory (DFT) method.

Methodology

Density Functional Theory (DFT) Calculations

In this work, we performed DFT calculations using the Vienna Ab initio Simulation Package (VASP)[4-8] using the projector augmented wave (PAW) pseudopotentials[9,10] , the Perdew-Burke-Ernzerhof (PBE) exchange-correlation functional[11,12] , and D3 dispersion corrections with Becke-Johnson damping[13,14] . Plane waves are included to an energy cutoff of 400 eV, spin polarization is turned off, and dipole corrections are applied in the direction normal to the surface. We first tested the calculations with the spin polarization turned on and later chose to turn it off because it did not significantly affect the results, a difference of 0.03 eV, and was more computationally achievable. The first Brillouin zones are sampled using 7x7x1 Monkhorst-Pack Gamma-centered k-point meshes[15] . Electronic energies are calculated self-consistently and considered to be converged when the difference between subsequent iterations falls below 10^{-6}eV. The geometry relaxations were performed in vacuum; therefore, all atoms in the supercell were allowed to relax. Geometries are considered converged when the forces on all atoms allowed to relax fall below 0.03 eV/Å. Charges are calculated from DFT using the DDEC6 atomic population analysis method[16].

The α-MoC surface was modeled by a 3x3 x 4 slab with the bottom two layers fixed for all adsorbates except O*, which had all layers fixed with the Pt and O allowed to move freely. To make the computation more tractable, neglecting surface restructuring, we decided that fixing all the surface layers for the case of O* to reduce the computational time. After performing some of the calculations, we discovered that it was computationally taking a while to converge; therefore, we decided that freezing the first two layers would help aid the computation. The calculated lattice parameter for the α-MoC surface was 10.26 Å, with an 8.98 Å x 8.98 Å x 27.78 Å supercell having

angles of α=90º, β=90º, γ=60º. Further information about the MoC surface and MoC with Pt (Figure 1) can be found in Supplemental Information 1 & 2.

(a) (b)

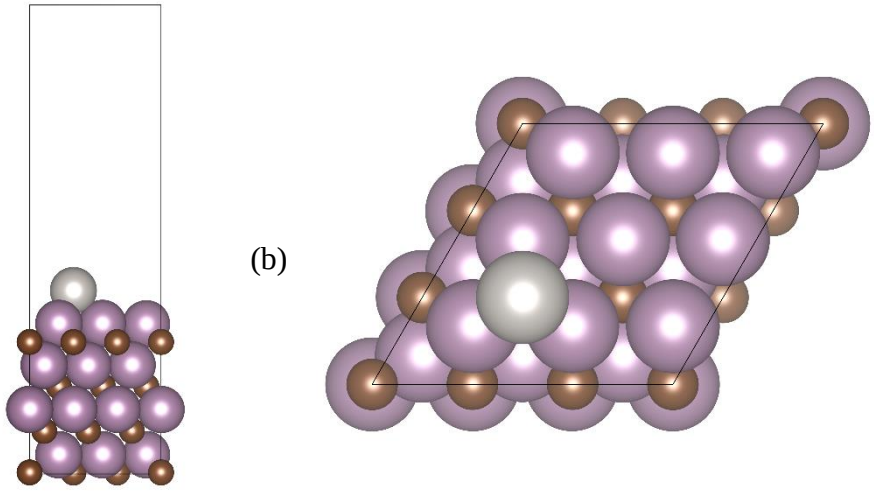

Figure 1: Supercell with single atom Platinum (a) front view (b) top view (Mo- Purple, C-brown, Pt-silver)

Results / Discussion

Binding Energies

To test the influence of the support on the chemistry of platinum, the table below compares how different supports affect the binding energy of different adsorbates for a similar system, taken from Cárcamo, et al.[17]. When CO is adsorbed on the MoC support, see Figure 2a, the binding energy is lower than when bound to just Pt_4 and the Al_2O_3 support; therefore, it has a lower binding strength. This result agrees with previous studies[18,19] and shows that MoC is a more favorable support for CO conversion. The MoC support would be a more favorable support for the CO conversion because it reduces the binding strength of CO in Pt_1/MoC and would require a lower reaction energy to remove the CO from the Pt. Sun et al. studied a Ir_1/ α-MoC structure and stated that it exhibits comparable WGS performance to the use of Au or Pt[1]. Their paper shows that the Ir_1/α-MoC has 1 to 2 orders of magnitude higher reaction rate compared to Ir_1/FeO_x and Ir_1/Al_2O_3 per single atom site[1]. What Sun et al.[1] observed is similar to the results we see, that the MoC support affects the binding strength of CO*. When looking at CO_2*, Figure 2b, we observe that CO_2 has a higher affinity for Pt/MoC when compared to Pt_4/Al_2O_3, Table 1. Looking at H*, Figure 1d, the binding strength decreases when the support is present; however, when MoC is the support, the binding strength is lower than when Al_2O_3 is the support. Leading to the conclusion that MoC is a more favorable support. When H_2O is the adsorbate (Figure 2c), the addition of MoC support does not change the binding strength from Pt-H_2O, but when it is Pt_4/Al_2O_3, the binding strength increases. Therefore, we observe that different supports have an effect on the WGS reaction.

Table 1: Adsorbate Binding Energies

Adsorbate	**Pt (111) $E_{Binding}$ [eV]**	**Pt/MoC $E_{Binding}$ [eV]**	**Pt_4/Al_2O_3 $E_{Binding}$ [eV]**
CO	-2.19	-1.98	-2.43‡
CO_2	-0.25	-0.67	-0.29‡
H_2O	-0.51	-0.50	-0.95‡
H	-0.68	-0.39	-0.64‡

Taken From: ‡ref(17) for comparison

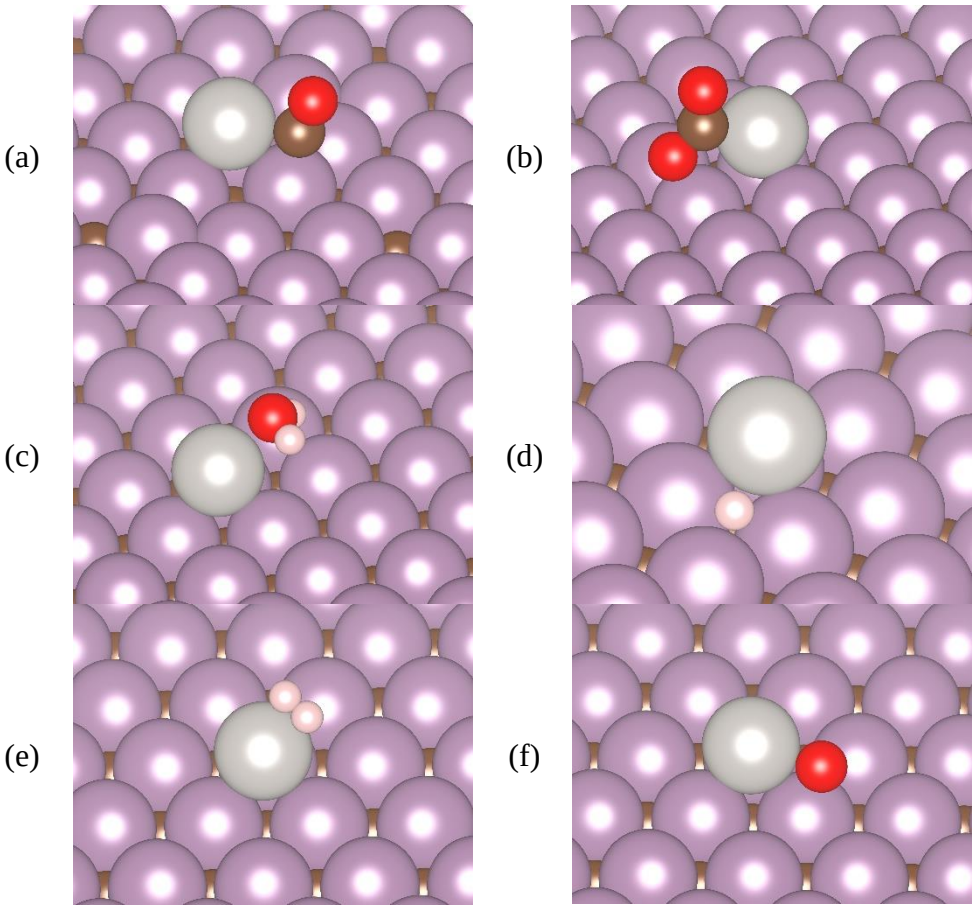

Figure 2: Lowest binding energy for (a) CO* (b) CO_2* (c) H_2O* (d) H* (e) H_2* (f) O* (Mo-Purple, C-brown, Pt-silver, O-red, H-pink)

Charge Calculations

To explore the influence of the support on the CO* binding, charges of the support (MoC), Pt/MoC, and CO bound to Pt/MoC were calculated and compared to a similar system, taken from Cárcamo, et al.[17] for CO bound to Pt, Pt_4/Al_2O_3, and CO bound to Pt_4/Al_2O_3, as shown in the below table. As seen in Table 2, there is an electron depletion from the MoC as it interacts with Pt and then CO bound to Pt. Similarly, we noticed that when Al_2O_3 is the support its electron density is reduced when CO bound to Pt, this interaction further reduces the electron density from the support. In both cases CO has a negative net charge but in MoC this net charge is larger than that of Al_2O_3. Therefore, we can see that the support modifies Pt's electronic structure, showing that the support is not an inert material and will have impact on the WGS reaction.

Table 2: Charges of MoC support, Pt/MoC, Pt/MoC with CO bound, Pt-CO, Pt_4/Al_2O_3, and Pt_4/Al_2O_3 with CO bound.

	Mo	**C**	**Support**	**Pt**	**CO**
MoC	0.9477	-0.9477	0	NA	NA
Pt/MoC	1.1738	-0.6338	0.3307	-0.3307	NA
Pt/MoC-CO*	0.9418	-0.9318	0.3616	-0.1924	-0.16916
Pt (111)	NA	NA	NA	-0.1399	0.1399
Pt_4/Al_2O_3	NA	NA	0.390‡	-0.390‡	NA
Pt_4/Al_2O_3-CO*	NA	NA	0.370‡	-0.250‡	-0.1194‡

Taken From: ‡ref(17) for comparison

Conclusion

For this report, we conclude that the support used in the WGS reaction would affect the reaction thermodynamics. The influence of the support can be seen in the binding strengths of the analyzed adsorbates. The adsorbate of focus was CO, and the binding strength decreased when MoC was the support. This decrease in binding strength compared to other supports leads to the conclusion that MoC is a more favorable support for CO conversion. The charge calculations comparing the support, Pt/MoC, and CO bound to Pt/MoC showed an electron depletion from the MoC as it interacts with Pt and CO. Therefore, we conclude that the support modifies the electronic structure of platinum making it less strongly bound to CO*. The overall conclusion we came to was that the support is not an inert material in the WGS reaction, and therefore, the support selection affects the performance of the WGS reaction.

Citations

1 Li Sun, Junkang Xu, Xiaoyan Liu, Botao Qiao, Lin Li, Yujing Ren, Qiang Wan, Jian Lin, Sen Lin, Xiaodong Wang, Hua Guo, and Tao Zhang, *ACS Catalysis* **2021** *11* (10), 5942-5950, DOI: 10.1021/acscatal.1c00231.

2 X. Zhang, M. Zhang, Y. Deng, *et al.* "A stable low-temperature H_2-production catalyst by crowding Pt on α-MoC." *Nature* **589**, 396–401 (2021). https://doi.org/10.1038/s41586-020-03130-6

3 J. Engelhardt, P. Lyu, P. Nachtigall, et al. "The Influence of Water on the Performance of Molydenum Carbide Catalysts in Hydrodeoxygenation Reactions: A Combined Theoretical and Experimental Study," ChemCatChem, 9, 185-1991 (2017), 10.1002/cctc.201700181.

4 G. Kresse and J. Hafner, "Ab initio molecular dynamics for liquid metals," Phys.Rev.B 47 (1), 558-561 (1993), 10.1103/PhysRevB.47.558.

5 G. Kresse and J. Furthmüller, "Efficiency of ab-initio total energy calculations for metals and semiconductors using a plane-wave basis set," Computational Materials Science 6(1), 15-50 (1996), https://doi.org/10.1016/0927-0256(96)0008-0.

6 G. Kresse and J. Furthmüller, "Efficient iterative schemes for ab initio total-energy calculations using a plane-wave basis set," Phys.RevB 54 (16), 11169-11186 (1996), 10.1103/PhysRevB.54.11169.

7 M. Hacene, A. Aniaux-Sedrakian, X. Rozanska, D. Klahr, T. Guignon and P. Fleurat-Lessard, "Accelerating VASP electronic structure calculations using graphic processing units," Journal of Computaional Chemistry 33 (32), 2581-2589 (2012), https://doi.org/10.1002/jcc.23096.

8 M. Hutchinson and M. Widom, “VASP on a GPU: Application to exact-exchange calculations of the stability of elemental boron,” Comput.Phys.Commun. 183 (7), 1422-1426 (2012), https://doi.org/10.1016/j.cpc.2012.02.017.

9 J.J. Mortensen, L.B. Hansen and K.W. Jacobsen, “Real-space grid implementation of the projector augmented wave method,” Physical Review B (3), (2005), 10.1103/physrevb.71.035109.

10 G. Kresse and D. Joubert, “From ultrasoft pseudopotentials to the projector augmented-wave method,” Phys.Rev.B 59(3), 1758-1775 (1999), 10.1103/PhysRevB.59.1758

11 John P. Perdew, Kieron Burke and Matthias Ernzerhof, “Generalized Gradient Approximation Made Simple,” Phys.Rev.Lett. 77 (18), 3865-3868 (1996), 10.1103/PhysRevLett.77.3865.

12 John P. Perdew, Kieron Burke and Matthias Ernzerhof, “Generalized Gradient Approximation Made Simple [Phys.Rev.Lett. 77, 3865 (1996)],” Phys.Rev.Lett. 78 (7), 1396 (1997), 10.1103/PhysRevLett.78.1396.

13 Stefan Grimme, Jens Antony, Stephan Ehrlich and Helge Krieg, “A consistent and accurate ab initio parametrization of density functional dispersion correction (DFT-D) for the 94 elements H-Pu,” J.Chem.Phys. 132 (15), 154104 (2010), 10.1063/1.3382344.

14 Stefan Grimme, Stephan Ehrlich and Lars Goerigk, “Effect of the damping function in dispersion corrected density functional theory,” J.Comput.Chem. 32 (7), 1456-1465 (2011), https://doi.org/10.1002/jcc.21759.

15 Hedrik J. Monkhorst and James D. Pack, “Special points for Brillouin-zone integrations,” Phys.Rev.B 13 (12), 5188-5192 (1976), 10.1103/PhysRevB.13.5188.

16 N.G. Limas, T.A. Manz, “Introducing DDEC6 atomic population analysis: part 4. Efficient parallel computation of net atomic charges, atomic spin moments, bod orders, and more,” RSC Adv., 8 (2018), 2678-2707, 10.1039/C7RA11829E.

17 García Cárcamo, Ricardo A. and Zhang, Xiaohong and Estejab, Ali and Zhou, Jiarun and Hare, Bryan J. and Sievers, Carsten and Sarupria, Sapna and Getman, Rachel B., Differences in Solvation Thermodynamics of Oxygenates at Pt/Al $_2$O $_3$ Perimeter Versus Pt(111) Terrace Sites Calculated Under Explicit Liquid Water. Available at SSRN: https://ssrn.com/abstract=4221335

18 L. Lin, S. Yao, R. Gao, *et al.* “A highly CO-tolerant atomically dispersed Pt catalyst for chemoselective hydrogenation.” *Nat. Nanotechnol.* **14**, 354–361 (2019). https://doi.org/10.1038/s41565-019-0366-5.

19 E. Chukwu, L. Molina, C. Rapp, et al. “Crowded supported metal atoms on catalytically active supports may compromise intrinsic activity: A case study of dual-site Pt/α-MoC catalysts,” Applied Catalysis B: Environmental, 329 (2023), https://doi.org/10.1016/j.apcatb.2023.122532.

Supporting Information

1. CONTCAR for MoC Surface

CONTCAR
1.00000000000000
8.9823646544999995 0.0000000000000000 0.0000000000000000
4.4911823272999998 7.7789559768999998 0.0000000000000000
0.0000000000000000 0.0000000000000000 27.7789554595999988
C Mo
36 36
Direct
0.7777777909999983 0.7777777909999983 0.0922814263789036
0.6666666870000029 0.0000000000000000 0.2807318523789064
0.5555555819999967 0.8888888959999974 0.1865917693789072
0.1111111120000032 0.4444444479999987 0.0922814263789036
0.0000000000000000 0.0000000000000000 0.2807318523789064
0.6666666870000029 0.6666666870000029 0.0035998473789078
0.0000000000000000 0.0000000000000000 0.0035998473789078
0.4444444479999987 0.1111111120000032 0.0922814263789036
0.7777777909999983 0.1111111120000032 0.0922814263789036
0.3333333429999996 0.3333333429999996 0.0035998473789078
0.3333333429999996 0.0000000000000000 0.0035998473789078
0.1111111120000032 0.1111111120000032 0.0922814263789036
0.0000000000000000 0.6666666870000029 0.0035998473789078
0.6666666870000029 0.0000000000000000 0.0035998473789078
0.6666666870000029 0.3333333429999996 0.0035998473789078
0.3333333429999996 0.6666666870000029 0.0035998473789078
0.3333333429999996 0.0000000000000000 0.2807318523789064
0.0000000000000000 0.6666666870000029 0.2807318523789064
0.0000000000000000 0.3333333429999996 0.0035998473789078
0.3333333429999996 0.6666666870000029 0.2807318523789064
0.6666666870000029 0.6666666870000029 0.2807318523789064
0.7777777909999983 0.4444444479999987 0.0922814263789036
0.1111111120000032 0.7777777909999983 0.0922814263789036
0.4444444479999987 0.7777777909999983 0.0922814263789036
0.2222222239999994 0.2222222239999994 0.1865917693789072
0.8888888959999974 0.2222222239999994 0.1865917693789072
0.2222222239999994 0.5555555819999967 0.1865917693789072
0.5555555819999967 0.2222222239999994 0.1865917693789072
0.8888888959999974 0.5555555819999967 0.1865917693789072
0.4444444479999987 0.4444444479999987 0.0922814263789036
0.2222222239999994 0.8888888959999974 0.1865917693789072
0.8888888959999974 0.8888888959999974 0.1865917693789072
0.3333333429999996 0.3333333429999996 0.2807318523789064
0.6666666870000029 0.3333333429999996 0.2807318523789064
0.0000000000000000 0.3333333429999996 0.2807318523789064

0.5555555819999967	0.5555555819999967	0.1865917693789072
0.0000000000000000	0.0000000000000000	0.1381814883789048
0.0000000000000000	0.6666666870000029	0.1381814883789048
0.6666666870000029	0.3333333429999996	0.1381814883789048
0.3333333429999996	0.0000000000000000	0.1381814883789048
0.6666666870000029	0.0000000000000000	0.1381814883789048
0.3333333429999996	0.3333333429999996	0.1381814883789048
0.2222222239999994	0.2222222239999994	0.3195955113789068
0.1111111120000032	0.7777777909999983	0.2313984583789050
0.7777777909999983	0.4444444479999987	0.2313984583789050
0.8888888959999974	0.8888888959999974	0.0414335983789087
0.1111111120000032	0.4444444479999987	0.2313984583789050
0.4444444479999987	0.7777777909999983	0.2313984583789050
0.5555555819999967	0.8888888959999974	0.0414335983789087
0.7777777909999983	0.7777777909999983	0.2313984583789050
0.6666666870000029	0.6666666870000029	0.1381814883789048
0.4444444479999987	0.4444444479999987	0.2313984583789050
0.0000000000000000	0.3333333429999996	0.1381814883789048
0.2222222239999994	0.8888888959999974	0.3195955113789068
0.2222222239999994	0.8888888959999974	0.0414335983789087
0.7777777909999983	0.1111111120000032	0.2313984583789050
0.1111111120000032	0.1111111120000032	0.2313984583789050
0.5555555819999967	0.5555555819999967	0.3195955113789068
0.5555555819999967	0.5555555819999967	0.0414335983789087
0.8888888959999974	0.5555555819999967	0.3195955113789068
0.3333333429999996	0.6666666870000029	0.1381814883789048
0.2222222239999994	0.5555555819999967	0.0414335983789087
0.5555555819999967	0.8888888959999974	0.3195955113789068
0.8888888959999974	0.8888888959999974	0.3195955113789068
0.8888888959999974	0.2222222239999994	0.0414335983789087
0.5555555819999967	0.2222222239999994	0.3195955113789068
0.5555555819999967	0.2222222239999994	0.0414335983789087
0.8888888959999974	0.2222222239999994	0.3195955113789068
0.2222222239999994	0.5555555819999967	0.3195955113789068
0.8888888959999974	0.5555555819999967	0.0414335983789087
0.4444444479999987	0.1111111120000032	0.2313984583789050
0.2222222239999994	0.2222222239999994	0.0414335983789087

2. CONTCAR of MoC with Pt

CONTCAR_MoC_334_Pt1_04
1.0000000000000000
8.9823646544999995 0.0000000000000000 0.0000000000000000
4.4911823272999998 7.7789559768999998 0.0000000000000000
0.0000000000000000 0.0000000000000000 27.7789554595999988
C Mo Pt
36 36 1
Direct
0.7779397318224892 0.7779397318224903 0.0919482330268587
0.2214294833608867 0.5571410632782191 0.1865001236945961
0.7779397318224894 0.4441205663550162 0.0919482330268587
0.1112912124359437 0.7774175901281197 0.0920107389276890
0.4441205663550156 0.7779397318224903 0.0919482330268587
0.2214294833608876 0.2214294833608876 0.1865001236945961
0.8886581867836394 0.2226836424327180 0.1863065735048832
0.6659764879007966 0.0010191860899685 0.2810373606939457
0.0010191860899685 0.6659764879007966 0.2810373606939457
0.5563291155333220 0.5563291155333220 0.1867996374990136
0.4441744323902577 0.4441744323902578 0.0915565103694721
0.2226836424327180 0.8886581867836394 0.1863065735048832
0.8886581867836394 0.8886581867836394 0.1863065735048832
0.3333333429999993 0.3333333429999998 0.2800732680537725
0.6659764879007966 0.3330043560092365 0.2810373606939457
0.0010191860899685 0.3330043560092365 0.2810373606939457
0.3330043560092365 0.6659764879007966 0.2810373606939457
0.5571410632782180 0.2214294833608876 0.1865001236945961
0.7774175901281197 0.1112912124359437 0.0920107389276890
0.3330043560092365 0.0010191860899685 0.2810373606939457
0.4441744323902577 0.1116511432194779 0.0915565103694721
0.5563291155333216 0.8873418289333445 0.1867996374990136
0.1116511432194779 0.4441744323902578 0.0915565103694721
0.0000000000000000 0.0000000000000000 0.2813765395608795
0.6666666870000030 0.6666666870000029 0.0032375492305616
0.0000000000000000 0.0000000000000000 0.0033860592772714
0.8873418289333438 0.5563291155333220 0.1867996374990136
0.6666666870000030 0.6666666870000029 0.2804204528187519
-0.0002459012611001 0.3334952236427506 0.0032559538666696
0.3333333429999993 0.3333333429999998 0.0030586087172351
0.3334952236427504 -0.0002459012611001 0.0032559538666696
0.1112912124359437 0.1112912124359437 0.0920107389276890
-0.0002459012611008 0.6667507076183512 0.0032559538666696
0.6667507076183501 -0.0002459012611001 0.0032559538666696
0.6667507076183489 0.3334952236427506 0.0032559538666696
0.3334952236427499 0.6667507076183512 0.0032559538666696
0.4441293998356698 0.4441293998356698 0.2309786905253907

0.1099583575327357 0.1099583575327357 0.2322544926713591
0.5563764242928519 0.5563764242928527 0.3197676376676692
0.5556207542992392 0.5556207542992396 0.0410122075875990
0.8872472114142875 0.5563764242928527 0.3197676376676692
0.3354438022427466 0.6642130793284371 0.1378535462708774
0.2222275173734769 0.5555449952530461 0.0409290254714403
0.8887585514015194 0.5556207542992396 0.0410122075875990
0.5563764242928519 0.8872472114142879 0.3197676376676692
0.8888796750979213 0.2222406658041491 0.0411677761994915
0.5539247005293700 0.2230376647353128 0.3209381607289457
0.0000000000000000 0.0000000000000000 0.1375335516624160
0.2222275173734769 0.2222275173734769 0.0409290254714403
0.5555449952530461 0.2222275173734769 0.0409290254714403
0.8885920694681525 0.2228158770636772 0.3200012157007763
0.2230376647353128 0.5539247005293700 0.3209381607289457
0.2222406658041483 0.8888796750979227 0.0411677761994915
0.4441293998356698 0.1117412083286632 0.2309786905253907
0.0003431484288250 0.3354438022427471 0.1378535462708774
0.8885920694681522 0.8885920694681532 0.3200012157007763
0.0003431484288248 0.6642130793284371 0.1378535462708774
0.6642130793284358 0.3354438022427471 0.1378535462708774
0.3354438022427471 0.0003431484288250 0.1378535462708774
0.6642130793284358 0.0003431484288250 0.1378535462708774
0.3333333429999993 0.3333333429999998 0.1382665385246076
0.2230376647353128 0.2230376647353128 0.3209381607289457
0.6666666870000030 0.6666666870000029 0.1381501037703631
0.7791048834075677 0.7791048834075677 0.2323417404149798
0.8888796750979207 0.8888796750979227 0.0411677761994915
0.1117412083286632 0.4441293998356698 0.2309786905253907
0.2228158770636768 0.8885920694681532 0.3200012157007763
0.7800832999345336 0.1099583575327357 0.2322544926713591
0.7791048834075676 0.4417902631848625 0.2323417404149798
0.4417902631848625 0.7791048834075677 0.2323417404149798
0.5556207542992387 0.8887585514015200 0.0410122075875990
0.1099583575327351 0.7800832999345352 0.2322544926713591
0.3333333429999993 0.3333333429999998 0.3911307134520743

3. INCAR for ISPIN1

System = INCAR_ISPIN1
NWRITE = 1
LWAVE = .FALSE. ! write WAVECAR?
LCHARG = .FALSE. #Set .True. Charge calculation will be performed otherwise set .False.
LAECHG = .FALSE. #Set .True. Charge calculation will be performed otherwise set .False.
LVTOT = .FALSE. ! write LOCPOT?

```
LSCAAWARE = .FALSE.

Electronic relaxation
IALGO  = 48    ! 8: CG, 48: DIIS algorithm for electrons
ENCUT  = 400
ALGO   = Fast
ISMEAR = 0     ! 0: Gaussian, electron smearing
SIGMA  = 0.100
PREC   = A
LREAL  = Auto
ISTART = 0
ICHARG = 2
#ADDGRID = T
NELM   = 75
# NELMDL = -8
# NELMIN = 6
EDIFF  = 1e-6
ISPIN  = 1     ! polarization?
# NUPDOWN= 1     ! excess electrons of majority spin
# MAGMOM = 0  0  0  0  5  5  5  5

Ionic relaxation
NSW    = 5000   ! # of steps in optimization (default 0!)
ISIF   = 2     ! 0: relax ions, 1,2:relax ions,calc stresses, 3:relax ion+cell
IBRION = 1     ! 1: quasi-NR, 2:CG algorithm for ions
NFREE  = 20    ! number of DIIS vectors to save
POTIM  = 0.5   ! reduce trial step in optimization
EDIFFG = -0.03

Dispersion
IVDW = 12


#Parallel #- optimized for GPUs on Palmetto. Only uncomment if you're submitting to GPUs.
#NCORE = 2
#KPAR = 2
#LPLANE = .TRUE.
#NSIM = 8
#NPAR = 8
```